An Improved Pulse Density Modulation Control for A Semi Active Rectifier in Wireless Power Transfer with LC/S Compensation

1st Veli Yenil
Department of Electrical-Electronics Engineering
(Pamukkale University)
Denizli, Turkey
veliyenil@pau.edu.tr
0000-0002-0257-5305

2nd Sevilay Cetin
Department of Biomedical Engineering
(Pamukkale University)
Denizli, Turkey
scetin@pau.edu.tr
0000-0002-9747-4821

2022 International Conference on Applied Electronics (AE) | 978-1-6654-9482-3/22/$31.00 ©2022 IEEE | DOI: 10.1109/AE54730.2022.9920024

***Abstract*—This paper proposes an improved pulse density modulation (PDM) control for a semi active rectifier (SAR) in wireless power transfer (WPT) with LC/S compensation. In order to improve the output regulation performance of the WPT converter, an improved pulse density modulation (PDM) is used, and its control signals are applied to the switches of the SAR. Based on the improved PDM control, the pulse sequence of the SAR is distributed more evenly compared to the traditional PDM. Thus, the output voltage ripple of the WPT converter is decreased and the output current ripple of the high frequency inverter (HFI) is decreased as well. The soft switching conditions can be achieved for both the SAR and HFI switches. In addition, since the control is applied only to the receiving side, there is no necessary for the communication devices. A simulation study is carried out to verify the performance of the improved PDM control and compared with the traditional PDM control. Based on the simulation results, the ripples of the output voltage as well as the output current ripples of the HFI are effectively reduced by using the improved PDM. Finally, the experimental results are presented to validate the effectiveness of the proposed control method.**

Keywords—LC/S compensation, pulse density modulation (PDM), wireless power transfer (WPT).

I. INTRODUCTION

Wireless power transfer (WPT) has come to the fore as it provides transfer to the power without any physical contact. In addition, it is convenient, efficient, and safe [1]. Because of these features, it has attracted attention in various applications such as consumer electronics, automatic guided vehicles (AGV), and electric vehicle charging.

An auxiliary dc-dc converter is generally used to achieve output voltage regulation at the secondary side of WPT converter [2]. However, an auxiliary dc-dc converter increases the system size and cost. Different transmitting side control methods have been proposed including duty, phase, or frequency control of the high frequency inverter (HFI). With these methods, the output voltage regulation can be achieved in the transmitting side. However, it is difficult to achieve soft switching condition of HFI, especially light load conditions.

To eliminate the use of dc-dc converter, as an alternative solution, active rectifier is proposed at the receiving side of the WPT converter [3]-[5]. Generally, by adjusting duty cycle or phase angle of the active rectifier, the output voltage regulation can be achieved. However, the active rectifier switches usually lose the soft switching condition with this method. In order to solve this problem pulse density modulation (PDM) method is proposed in [6],[7] for the active rectifier at the receiving side. The PDM control can provide soft switching condition of semi active rectifier (SAR). It can also be adopted to the HFI at the transmitting side [8]. However, in PDM control, when the load decreases, current ripples are increased and therefore the optimization of pulse distribution is required.

In this study, an improved PDM control approach is proposed to regulate the output voltage of the WPT converter using SAR. The proposed WPT converter can achieve the output voltage regulation without depending on communication device between the transmitting and receiving side. Compared to the traditional PDM, proposed PDM effectively reduce the output current ripples of the HFI, and the output voltage ripples of the SAR. In addition, the soft switching condition of the SAR is achieved over a wide load range. The performance of the proposed PDM controlled WPT converter is verified by a simulation study. The simulation study is carried out with 1.05 kW output power for the full load condition. In the simulation work, traditional PDM and proposed PDM control are compared with each other in terms of current and voltage ripples performance. An experimental prototype is also built to verify the performance of the proposed method. According to experimental results, the proposed method shows better current ripple performance compared to the traditional PDM method.

II. THEORETICAL ANALYSIS OF THE WPT SYSTEM

The LC/S compensation WPT converter with SAR is shown in Fig.1. L_P and L_S are the self-inductances of magnetic coupler, respectively. M denotes corresponding mutual inductance of the magnetic coupler. While the HFI composed of four MOSFETs (Q_1-Q_4) which invert to dc voltage to high frequency ac voltage, the SAR is composed of D_5 and D_6 diodes and Q_7 and Q_8 MOSFETs. L_r is the transmitting resonant inductor. C_p and C_s are the transmitting and receiving side resonant capacitors, respectively. C_F is the output capacitor and R_o, is the load. V_{ab} is the output voltage of the transmitting side HFI, V_{cd} is the input voltage of the SAR at the receiving side. V_o and i_o is the dc side voltage and current of the WPT converter, respectively.

978-1-6654-9482-3/22/$31.00 ©2022 IEEE

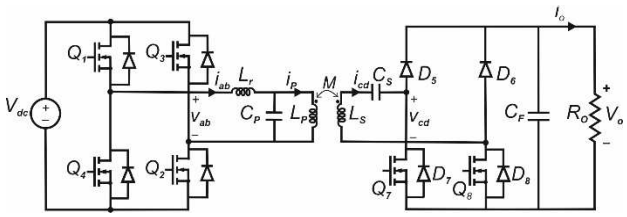

Fig. 1. WPT system with LC/S compensation network.

The equivalent model of LC/S compensation network with the fundamental approximation is shown in Fig. 2. $\mathbf{V}_{ab}$ is the fundamental component of v_{ab}. $\mathbf{V}_{cd}$ is the fundamental component of v_{cd}. R_e is the equivalent resistance of load. ω is the operation frequency of the WPT converter.

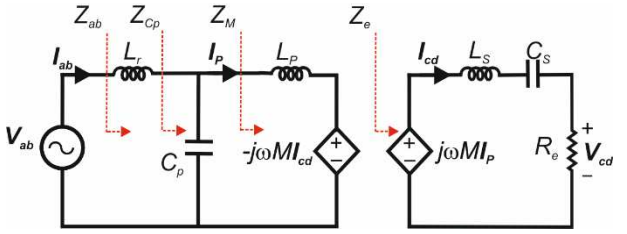

Fig. 2. AC equivalent model of the LC/S network.

The voltage equations of the transmitting and receiving side can be derived from Fig.2

$$V_{ab} = \boldsymbol{I}_{ab}(j\omega L_r + \frac{1}{j\omega C_P}) - \boldsymbol{I}_P \frac{1}{j\omega C_S} \quad (1)$$

$$j\omega M \boldsymbol{I}_P = \boldsymbol{I}_{cd}(j\omega L_S + \frac{1}{j\omega C_S}) + \boldsymbol{I}_{cd} R_{eq} \quad (2)$$

Where R_s can be determined by

$$R_e = \frac{\boldsymbol{V}_{cd}}{\boldsymbol{I}_{cd}}. \quad (3)$$

The WPT converter with SAR is shown in Fig 1. In the PDM control, ZVS and ZCS conditions are achieved over a wide load range. Therefore, switching losses of the SAR can be eliminated. In order to achieve higher efficiency performance of the WPT converter with SAR, the PDM method is preferred and improved in this study.

Fig. 3 and Fig 4 show the traditional PDM and proposed PDM control patterns for the SAR, respectively. With the proper implementation of PDM control, the ZVS turn on for the switches of SAR (Q_7-Q_8) can be achieved over the wide load range. Furthermore, all the SAR diodes (D_5 - D_8) turn-on with ZCS. Because of the long waiting time of the traditional PDM as given Fig. 3, the output voltage regulation performance deteriorates, and the current ripple increases. Due to these reasons, the traditional PDM pattern replaced with the proposed PDM pattern as given in Fig. 4. So, the proposed PDM pattern is adapted to the SAR. In PDM control, the output voltage regulation is provided by adjusting the PDM duty of the switches of the SAR during the one PDM period T. The SAR is always operated with the help of the proposed PDM pattern.

The traditional PDM control for the SAR has two operation modes which is named as active mode and passive mode. If the SAR operated with passive mode, the receiving side is shorted. While the current flows through Q_7 and D_8 in the positive half cycle of v_{cd}, and the current flows through Q_6 and D_7, in the negative half cycle of v_{cd}. Therefore, the load power is zero in this mode. The load fed by only the output filter capacitor and the Re is equal to 0. If the SAR works at active mode, the conventional diode bridge mode starts to work. So, the power producing in transmitting side is delivered to load with the help of (D_5- D_8) and (D_6- D_7) diodes respectively. In this mode R_e is equal to $8R_o/\pi^2$.

In addition to the active and passive modes, the proposed PDM has a new mode called semi-mode. In the active and passive operation modes, the SAR works similarly to traditional PDM. On the other hand, in the semi mode operation, the input voltage of SAR has a positive and negative part pulses unlike traditional PDM. This is because to transient state is introduced between the active and passive modes of operation of SAR which is used to distribute the pulse sequence more optimized. The waiting time of the passive mode operation is reduced with the help of semi mode. Thus, the output voltage is regulated more precisely.

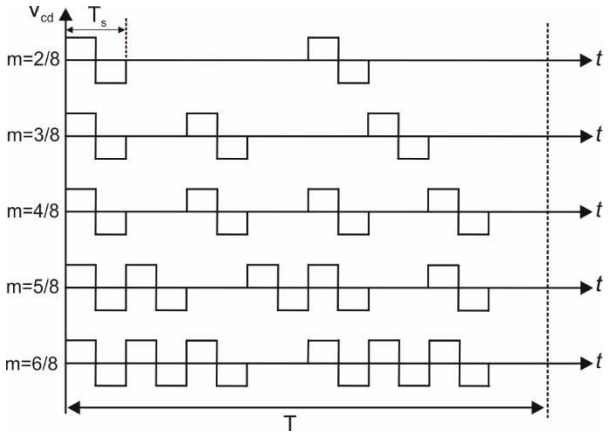

Fig. 3. The traditional PDM input voltage pattern of SAR

The peak input voltage of the SAR can be calculated as

$$V_2 = \frac{4V_L}{\pi} m. \quad (5)$$

Where m is the pulse density for the traditional PDM, and it is defined by:

$$m = \frac{T_S}{T}. \quad (6)$$

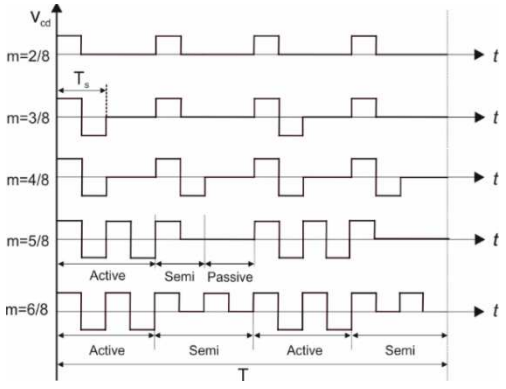

Fig. 4. The proposed PDM input voltage pattern of SAR

According to the Fig.4, for the proposed PDM, the m defined by:

$$m = k\frac{T_S}{T}. \tag{7}$$

Where k is the total number of the positive and negative part pulse of the v_{cd} in the one PDM period T.

III. Simulation Results

A simulation study is performed to test the proposed PDM control. The parameters of the LC/S compensated WPT system using SAR are listed in Table I. The resonant network parameters are determined according to the load independent CC output with zero phase angle condition as given in [9]. The output voltage and current are both constants at 85 kHz. With the use of proposed PDM, the output voltage regulation performance is improved for the SAR compared to the traditional PDM. In addition, the current ripple of the HFI is significantly reduced. The soft switching condition for the switches of SAR is also achieved.

TABLE I. The WPT Converter Parameters

Parameters	Value	Parameters	Value
P_O	1.05 kW	k	0.25
V_{in}	200 V	L_P–L_S	290 μH
V_O	210 V	L_1	242 μH
I_O	5 A	C_P	26.6 nF
ω_o	85 kHz	C_S	13.6 nF

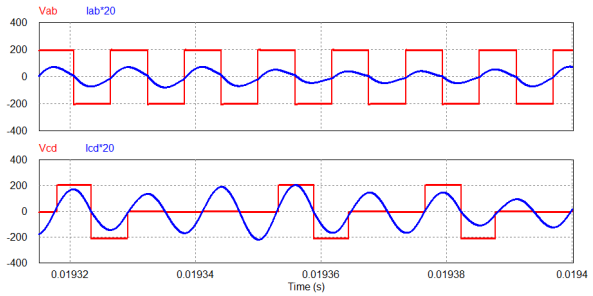

Fig. 5. Simulated waveforms of the voltage and current across the HFI and the SAR, with traditional PDM under the 393 W load power.

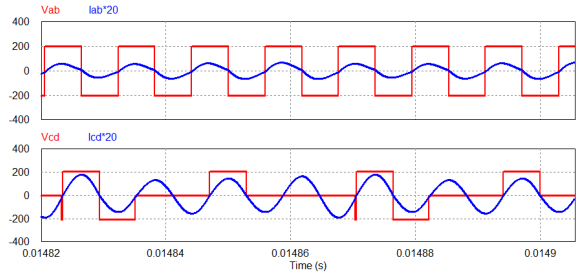

Fig. 6. Simulated waveforms of the voltage and current across the HFI and the SAR, with proposed PDM under the 393 W load power.

When the system operates at 210 V output voltage regulation for the 393 W load power, the simulated waveforms of the output voltage and current of HFI and the input voltage and current of the SAR are depicted in Fig. 5. and Fig. 6. According to Fig. 5 and Fig. 6, the input current ripple of the HFI with the improved PDM is lower than the traditional PDM. Fig. 7 and Fig. 8 show the output voltage ripple waveform. From Fig. 7 and Fig. 8, it can be seen that the output voltage ripple of the traditional PDM is higher than the proposed PDM for the 393 W load power.

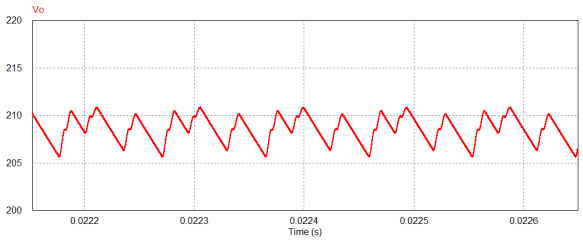

Fig. 7. The output voltage ripple waveform of the WPT converter with traditional PDM, V_o=210 V under the 393 W load power.

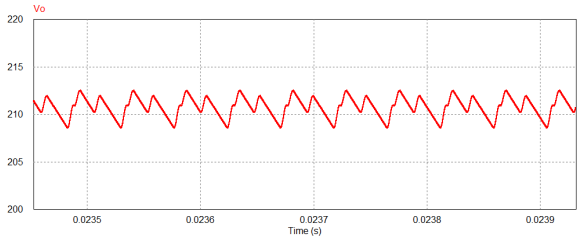

Fig. 8. The output voltage ripple waveform of the WPT converter with proposed PDM, V_o=210 V under the 393 W load power.

In order to make a performance comparison for both traditional and proposed PDM control, the experimental study is also performed under the 393 W load power. Experimental waveforms of the output voltage and current of HFI and the input voltage and current of the SAR are shown in Fig. 9 and Fig 10. As can be seen from these figures, the input current ripple is effectively reduced. It can also be realized that the output voltage ripple is reduced.

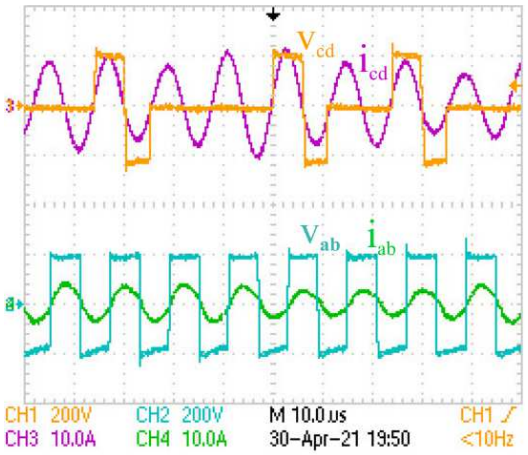

Fig. 9. Experimental waveforms of the voltage and current across the HFI and the SAR, with traditional PDM under the 393 W load power.

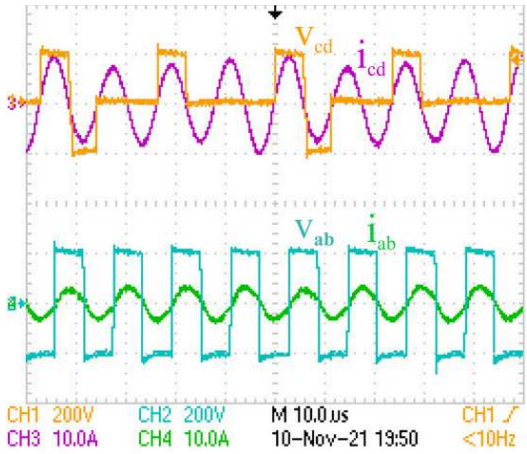

Fig. 10. Experimental waveforms of the voltage and current across the HFI and the SAR, with proposed PDM under the 393 W load power.

In comparison with the other control methods such as phase-shift control, the soft switching condition of SAR switches cannot be provided for a wide load condition. Therefore, high switching loss occurs for SAR switches resulting in low system efficiency.

IV. Conclusion

This paper proposes an improved PDM control for the LC/S compensated WPT converter with SAR. Based on the improved PDM strategy, the pulse sequence distribution of the SAR is more evenly compared to the traditional PDM. The output voltage regulation performance of the WPT converter with SAR is increased by using proposed PDM. Furthermore, the soft switching condition is achieved for the switches of SAR. According to the simulation and experimental results, the output voltage ripple of the proposed PDM and the current ripple of HFI are effectively reduced compared to the traditional PDM control at 393 W load power.

Acknowledgment

This work is supported by Pamukkale University under grant number 2020FEBE034.

References

[1] G. S. Li and C. C. Mi, "Wireless power transfer for electric vehicle applications," IEEE J. Emerg. Sel. Topics Power Electron., vol. 3, no. 1, pp. 4–17, Mar. 2015.

[2] Y. Yang, W. Zhong, S. Kiratipongvoot, S. Tan, and S. Y. R. Hui, "Dynamic improvement of series−series compensated wireless power transfer systems using discrete sliding mode control," IEEE Trans. Power Electron., vol. 33, no. 7, pp. 6351–6360, Jul. 2018.

[3] K. Colak, E. Asa, M. Bojarski, D. Czarkowski, and O. C. Onar, "A novel phase-shift control of semibridgeless active rectifier for wireless power transfer," IEEE Trans. Power Electron., vol. 30, no. 11, pp. 6288–6297, Nov. 2015.

[4] T. Diekhans and R. W. De Doncker, "A dual-side controlled inductive power transfer system optimized for large coupling factor variations and partial load," IEEE Trans. Power Electron., vol. 30, no. 11, pp. 6320–6328, Nov. 2015.

[5] H R. Mai, Y. Liu, Y. Li, P. Yue, G. Cao, and Z. He, "An active-rectifier-based maximum efficiency tracking method using an additional measurement coil for wireless power transfer," IEEE Trans. Power Electron., vol. 33, no. 1, pp. 716–728, Jan. 2018.

[6] M. Fan, L. Shi, Z. Yin, and Y. Li, "A novel pulse density modulation with semi-bridgeless active rectifier in inductive power transfer system for rail vehicle," CES Trans. Elect. Mach. Syst., vol. 1, no. 3, pp. 397–404, Dec. 2017.

[7] S. Cetin and V. Yenil, "Performance Evaluation of Constant Voltage Charging Mode of Secondary Side Controlled Inductive Power Transfer System," 2021 International Aegean Conference on Electrical Machines and Power Electronics (ACEMP) & 2021 International Conference on Optimization of Electrical and Electronic Equipment (OPTIM), 2021, pp. 315-318.

[8] G. Bal, S. Oncu, N. Ozturk and K. Unal, "An Application of PDM Technique for MPPT in Solar Powered Wireless Power Transfer Systems," 2021 10th International Conference on Renewable Energy Research and Application (ICRERA), 2021, pp. 305-309.

[9] Y. Wang, Y. Yao, X. Liu, D. Xu, and L. Cai, "An LC/S compensation topology and coil design technique for wireless power transfer," IEEE Trans. Power. Electron., vol. 33, no. 3, pp. 2007–2025, Mar. 2018.